Renewable Energy Vol. 1, No. 5/6, pp. 595–607, 1991
Printed in Great Britain.

DESIGN ANALYSIS OF CORRUGATED AND FLAT PLATE SOLAR AIR HEATERS

C. CHOUDHURY and H. P. GARG
Centre for Energy Studies, Indian Institute of Technology, Hauz Khas, New Delhi-110016, India

(*Received* 23 *August* 1991; *accepted* 12 *September* 1991)

Abstract—A detailed theoretical parametric analysis has been made on corrugated and flat plate solar air heaters of five different configurations. The analysis involves investigating the effects of the air flow velocities (or the air channel depths) on the air temperature increment, the system efficiency and the pressure drop experienced by the flowing air for different air channel lengths and different specific mass flow rates of air. The design analysis and the curves discussed in the article are intended to enable a designer to construct economical and efficient solar air heaters with technically logical air passage dimensions.

1. INTRODUCTION

The commercial acceptability of a solar air heating system depends on its performance efficiency and cost-effectiveness. The key parameter responsible for increasing the efficiency of such a system is the overall heat transfer coefficient between the absorber and the flowing air. This parameter, for a fixed specific mass flow rate of air through the heater channel, can be varied by varying the air velocity or the air channel depth which, in turn, causes a variation in the pressure drop experienced by the air stream in passing through the collector channel. If no upper bound is placed on the pressure drop in the system, the convective heat transfer coefficient (between the absorber and the flowing air) can be made arbitrarily large by the proper choice of the flow passage dimension. However, a cost-effective design consideration of the system provides constraints on the pressure drop and hence on the flow passage depth of the system. If the material cost of the collector is fixed, then for a fixed specific mass flow rate of air, the economics of the system are governed by the cost of the pumping power expended in the collector which depends on (increases with) the pressure drop in the system. A consideration of these points suggests the existence of optimum air flow passage dimension that corresponds to efficient and cost-effective design of the system.

A review of solar heating literature [1–4] reveals that flat and corrugated plate solar air heaters have received considerable attention for space heating, agricultural drying and to some extent, water heating applications. However, little has been published on the effect of the air flow passage dimension on the efficiency and the pressure drop and hence on the cost-effectiveness of the system. Charters [5] in 1971 examined the optimization of aspect ratio of the rectangular flow passage from the point of view of minimizing the cost for a fixed pumping power. Hollands and Schewen [6] in 1981 studied the effect of the dimensions of the air flow passage on the heat transfer coefficient between the absorber and the flowing air for fixed pressure drop values. They used rectangular and triangular flow passage in plate-type air heating collectors. Choudhury *et al.* [7] investigated the effects of the air flow passage dimension on the air temperature increment and the efficiency of an uncovered corrugated plate air heater. In the present study, attempts have been made to examine theoretically the effects of the air flow passage dimensions (length and depth) on the collector efficiency, the air temperature increment and the pressure drop in the system for different fixed specific mass flow rates of air. Five different configurations of corrugated and flat plate solar air heaters were used.

2. THEORETICAL ANALYSIS

Figure 1(a) (a–e) shows schematically the cross-sectional views of the solar air heaters investigated in the present work. In all the configurations, the air heaters are comprised of three plates. Plate 1, the upper-most plate, act as the cover in all the configurations, plate 2, the middle plate, is the inner cover in Types I, II and III and absorber in Types IV and V, and plate 3, insulated at the bottom, is the rear plate which is the absorber in Types I, II and III and wooden sheet in Types IV and V. In all the configurations, the air flows through the passage between

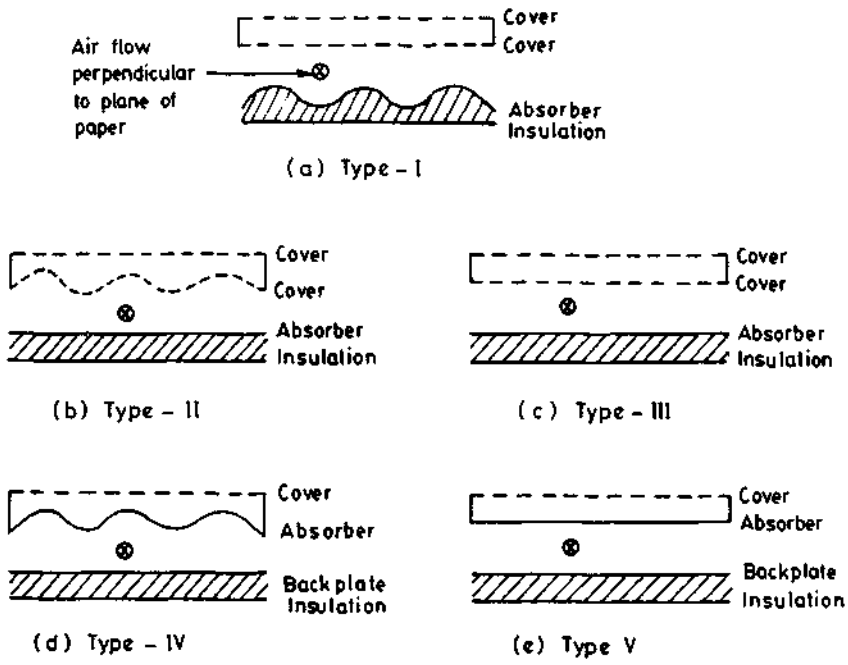

Fig. 1(a). Schematic views of the solar air heaters.

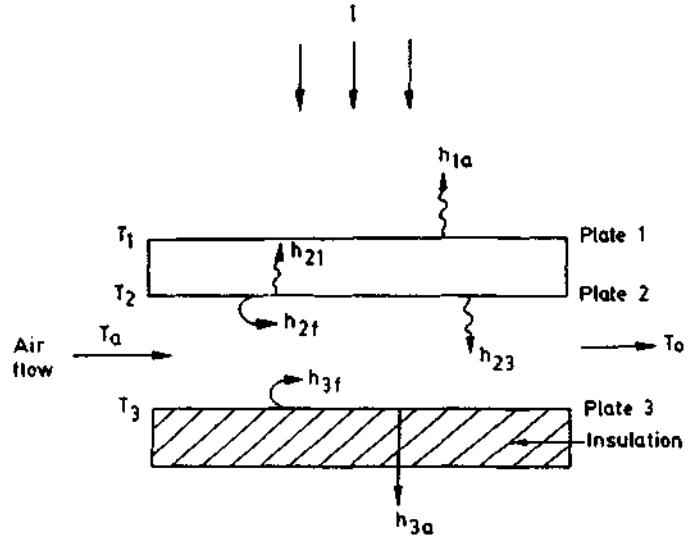

Fig. 1(b). Coefficients of various heat transfer in the solar air heaters.

the middle and the rear plate and provides the heat transfer. The various heat transfer coefficients at different components of the air heaters are shown in Fig. 1(b). In the analysis, the heat transfer is considered to be steady state, equal ambient temperatures are assumed at the front and the rear of the collector and the inlet air temperature is assumed to be the same as the ambient temperature. The energy balance equations for the plates and the flowing air in these configurations can be written as:

$$S_1 I + h_{21}(T_2 - T_1) = h_{1a}(T_1 - T_a) \quad (1)$$

$$S_2 I = h_{21}(T_2 - T_1) + h_{23}(T_2 - T_3) + h_{2f}(T_2 - T_f) \quad (2)$$

$$S_3 I = h_{32}(T_3 - T_2) + h_{3f}(T_3 - T_f) + h_{3a}(T_3 - T_a) \quad (3)$$

$$(\dot{M}_f C_f / W)(dT_f/dy) = h_{2f}(T_2 - T_f) + h_{3f}(T_3 - T_f). \quad (4)$$

The boundary conditions are:

$$T_f = T_a \quad \text{at} \quad y = 0$$

$$T_f = T_o \quad \text{at} \quad y = L.$$

In the above equations:

$$S_1 = \alpha_1$$

$$S_2 = \tau_1 \alpha_2$$

and

$$S_3^* = \tau_1 \tau_2 \alpha_3.$$

For the corrugated absorber (cover), since the actual surface area absorbing (transmitting) the incident radiation is larger than the nominal area used for estimating the specific mass flow rate of air and since a part of the radiation is absorbed (transmitted) by multiple reflection on the absorber (glass) surface, the effective value of $\alpha(\tau)$, the total solar absorptance (transmittance) for the corrugated absorber (cover) in the computation is assumed to be 0.95 (0.95) where as that for the flat absorber (cover) is 0.90 (0.90).

Solving eqs (1)–(3) for T_1, T_2 and T_3 and integrating eq. (4) (after substituting for T_2 and T_3) within the limits $T_f \to T_a$ to T_o as $y \to 0$ to L, the outlet air temperature T_o was obtained as:

$$T_o = (T_i + P_{18}/P_{19}) \exp(P_{19} L W / \dot{m}_f C_f) - P_{18}/P_{19}. \quad (5)$$

The coefficients Ps are defined in the appendix.

The efficiency of the collector was then obtained by using the relation:

$$\eta = \frac{\dot{m}_f C_f (T_o - T_a)}{I}. \quad (6)$$

Heat transfer coefficients

The radiative and the wind related convective heat transfer coefficient h_{1a}, the radiative and the natural convective heat transfer coefficient h_{21}, the radiative heat transfer coefficient h_{23} and the conductive heat transfer coefficient h_{3a} were obtained by using the standard heat transfer relations summarized in Duffie and Beckman [3].

The forced convective heat transfer coefficients h_{2f} and h_{3f} were obtained by using the relation derived by Tan and Charters [8] which includes the effects of the entrance and exit length in the air flow passage and which is given by:

$$h = Nu\, K/D \quad (7)$$

$$Nu = Nu_\infty (1 + MD/L) \quad (8)$$

where

$$Nu_\infty = 0.0182 Re^{0.8} Pr^{0.4} \quad (9)$$

$$Re = \rho V D/\mu \quad (10)$$

$$M = 14.3(\log N - 7.9) \quad (11)$$

with

$$N = L/D \quad \text{if} \quad 0 < L/D \leqslant 60$$

$$= 60 \quad \text{if} \quad L/D > 60.$$

To account for the heat transfer to the flowing air from the corrugated plate, the right-hand side of eq. (7) is multiplied by the corrugation factor β.

Pressure drop

When air flows through the channel in the air heater, owing to friction, the air pressure drops along the length of the flow channel. If the effects of the channel entrance and exit, of surface roughness and of the compressibility of the air are neglected, the pressure drop ΔP can be computed from the relation:

$$\Delta P = 2f(\rho V^2) L/D \quad (12)$$

where the friction factor f, for turbulent flow, is given by [6, 9]:

$$f = 0.059 Re^{-0.2}. \quad (13)$$

Numerical values of different parameters, i.e. T_o, η etc., were computed corresponding to an ambient temperature of 300 K, solar flux of 900 W/m^2 and wind speed of 1.5 m/s. It may also be noted that eqs (8)–(13) were used for computing h_{2f}, h_{3f} and ΔP for turbulent as well as transition flow regimes and that no theoretical results were obtained in the laminar flow region.

3. RESULTS AND DISCUSSION

The computed values of the efficiency for different specific mass flow rates of air through the channel in the Type I air heater are plotted against the flow

* S_3 for Types IV and V collectors is zero.

velocity in Fig. 2. With an increase in the air mass flow rate, the curves show an increase in the efficiency, which is very rapid at lower flow rates and less rapid at higher flow rates. In addition, as may be noted, for a fixed specific air flow rate and a fixed collector length, the efficiency increases with increase in the air velocity, initially rapidly and then slowly. This can be attributed to the fact that larger air velocities with shallower air channel depths cause larger heat transfer to the flowing air (Fig. 3) resulting in higher efficiency of the system. However, the dependence of efficiency on air velocity is more predominant at higher mass flow rate than at lower flow rates. The relationship between the air temperature increment and the system efficiency for different air flow rates and air velocities for the five different configurations of the air heaters is shown in Figs 4–8. The curves illustrate that with increase in the temperature increment of the flowing air, the efficiency of the air heaters decreases. It is also revealed that the speed of the air is most important in determining the efficiency at higher air flow rates and the temperature rise at lower flow rates. Therefore, the temperature rise of the flowing air can be increased by decreasing the air flow rate per unit area and the loss in efficiency at lower flow rates can be avoided by increasing the air speed or by decreasing the channel depth in the air heater until the pressure drop experienced by the flowing air is the maximum that can be tolerated.

The variation in efficiency with the air channel depth for different collector lengths is displayed in Figs 9–13 for different specific mass flow rates of air through the heaters. A comparison of efficiencies in these figures indicates that at a fixed specific air flow rate and a fixed air velocity, the system efficiency decreases with increase in the air channel length. This effect is more predominant at lower air velocities. The curves also illustrate that for a fixed specific air flow rate and a fixed air channel length, the efficiency increases with increased air velocity (or decrease in

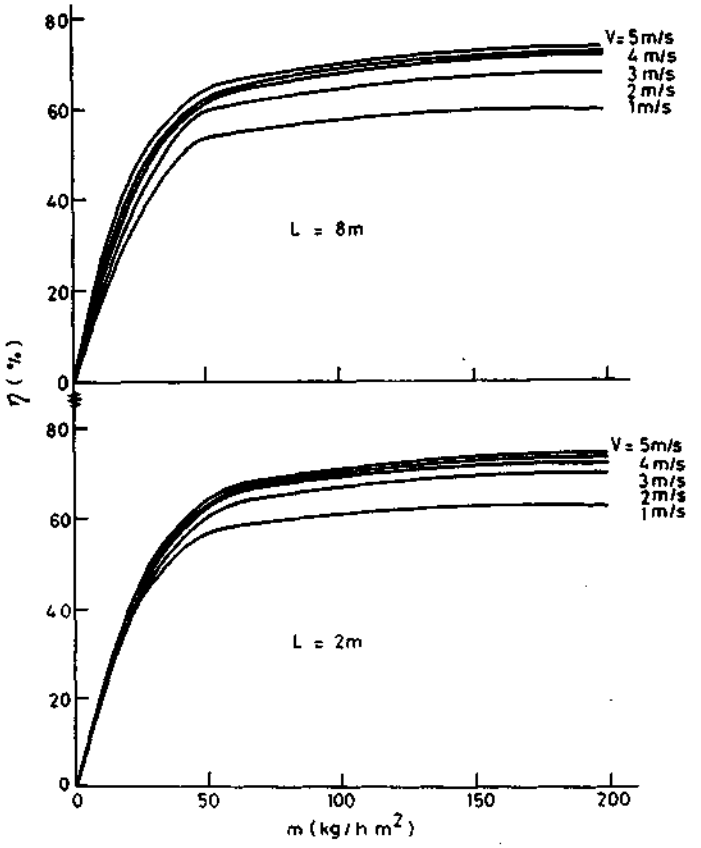

Fig. 2. Efficiency as function of the specific mass flow rates of air for Type I air heater.

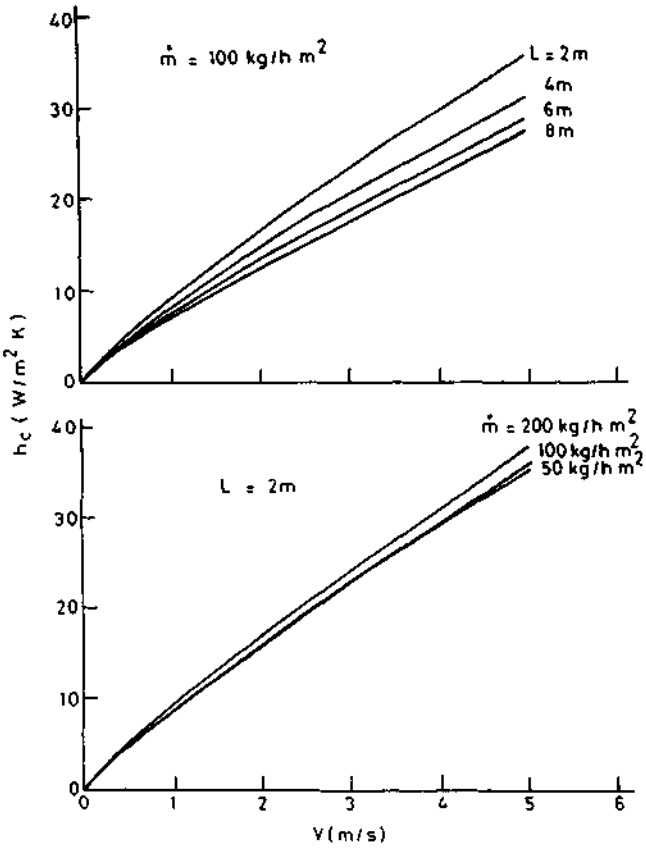

Fig. 3. Effect of air velocity on the coefficient of convective heat transfer between corrugated absorber and flowing air.

air channel depth). This effect is more predominant for longer air flow channels with higher specific air flow rates.

If no upper bound is placed on the air speed, the efficiency of the systems can be increased arbitrarily by the proper choice of the air channel dimension. However, as has been mentioned earlier, too large an air velocity and too small an air channel depth result in excessive pressure drop in the system and hence in excessive fan running costs. A consideration of this point suggests the existence of air flow channel with optimum dimensions which would correspond to efficient and cost-effective designs of the systems.

Figures 14 and 15 show the variation of pressure drop in the air flow passage as function of air passage depth for different heater lengths and different specific mass flow rates of air through the heater channel. An analysis of the values in different figures suggests that at 50 kg/h m^2 specific flow rate of air in a 6 m long air channel, by increasing the air velocity from 2 to 4 m/s (or decreasing the air channel depth from 3.5 to 1.75 cm), the efficiency increases by 3–6% in different collector types (Figs 9–13) whereas the pressure drop rises from 10 to 70 Pa (Fig. 14), thus increasing the pumping power expended by about 7 times. Similarly, at 150 kg/h m^2 air flow rate for a 6 m long collector, the increase in air velocity from 2 to 4 m/s (i.e. decrease in air channel depth from 10.5 to 5.2 cm) increases the efficiency by 4–7% (Figs 9–13) whereas the pressure drop and hence the pumping power by more than 7 times (Fig. 15).

To obtain systems with low pressure drops and improved efficiencies, proper dimensions of the air flow passages, such as their length and depth, can be chosen from the sets of curves as plotted in Figs 14 and 15, if fixed values of the pressure drop and the air flow rate (by requirement of the air temperature increment) are assumed at the beginning of the optimization procedure. For this purpose, depending on the dimension of the space available for installation,

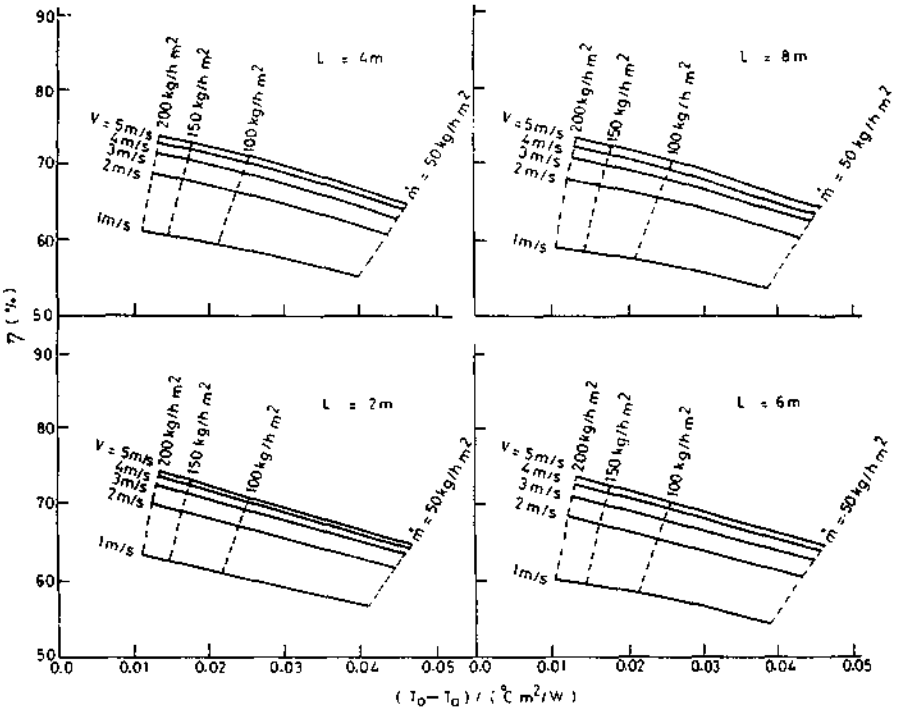

Fig. 4. Efficiency as a function of air temperature increment per unit incident flux for different air velocities in the Type I air heater.

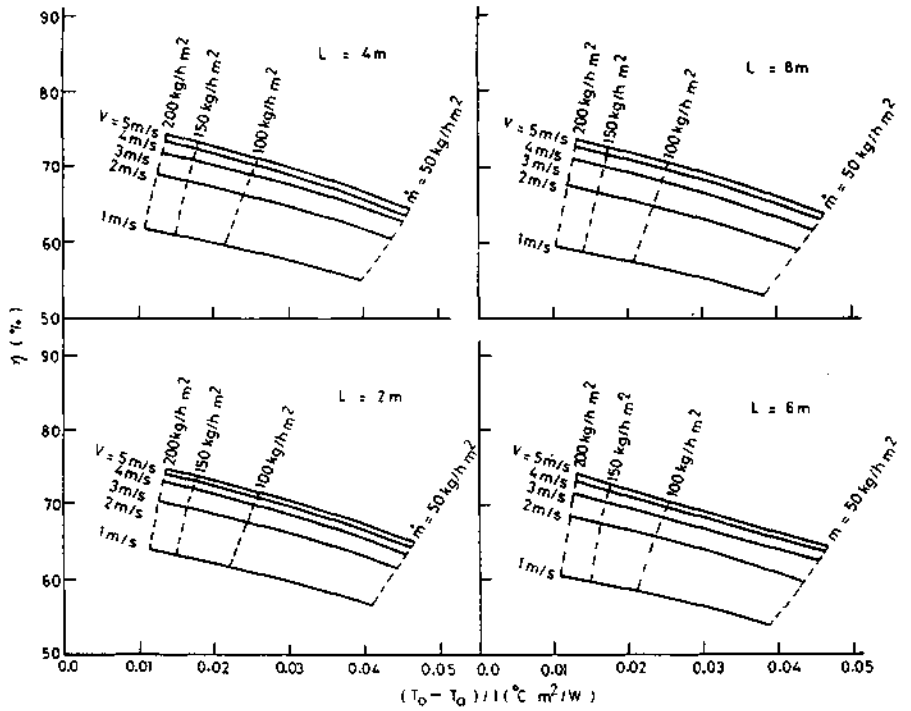

Fig. 5. Efficiency as a function of air temperature increment per unit incident flux for different air velocities in the Type II air heater.

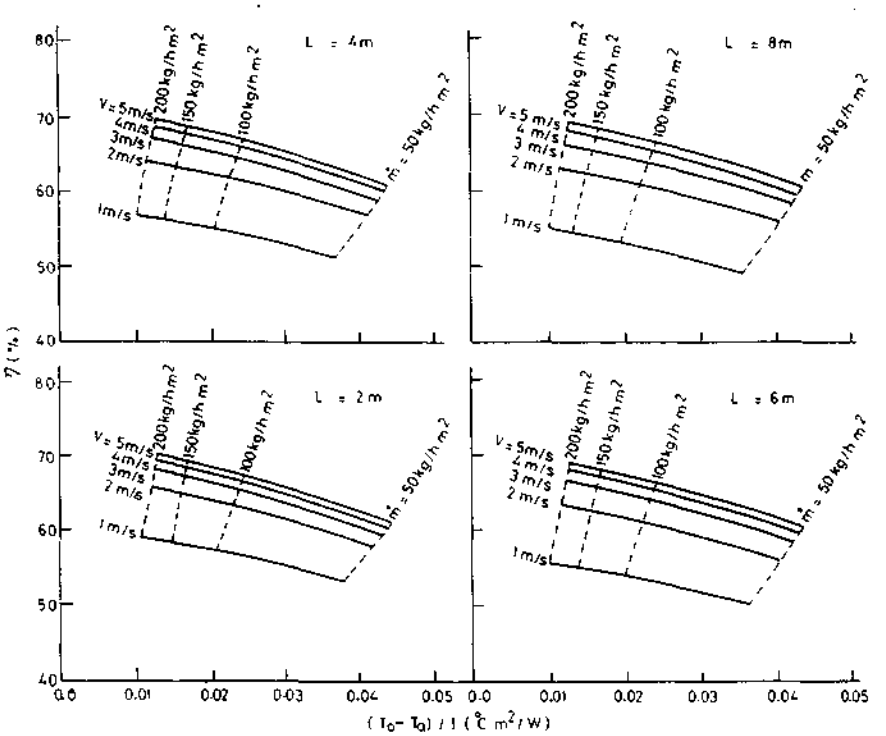

Fig. 6. Efficiency as a function of air temperature increment per unit incident flux for different air velocities in the Type III air heater.

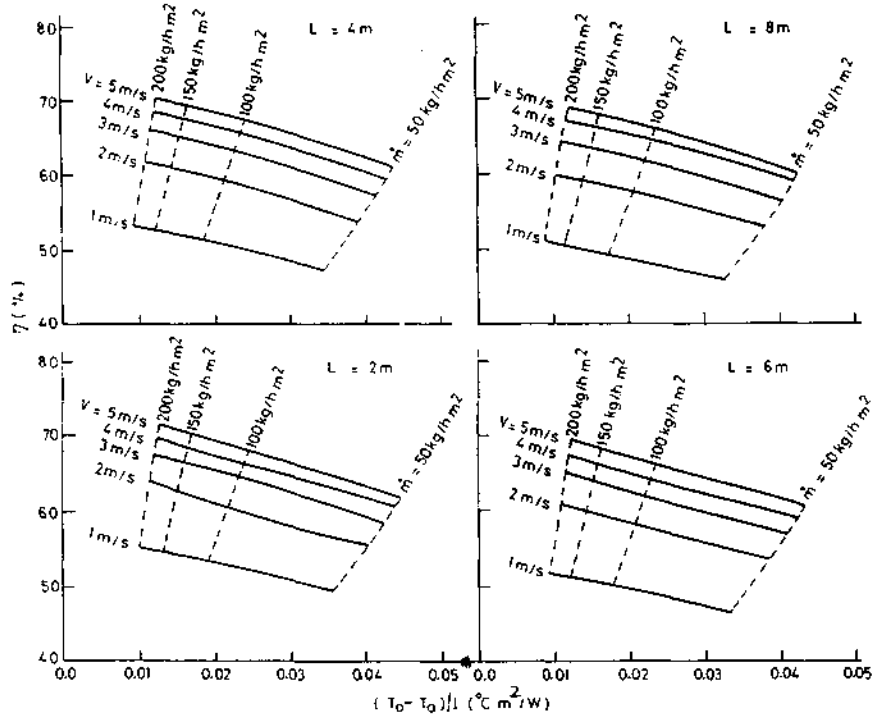

Fig. 7. Efficiency as a function of air temperature increment per unit incident flux for different air velocities in the Type IV air heater.

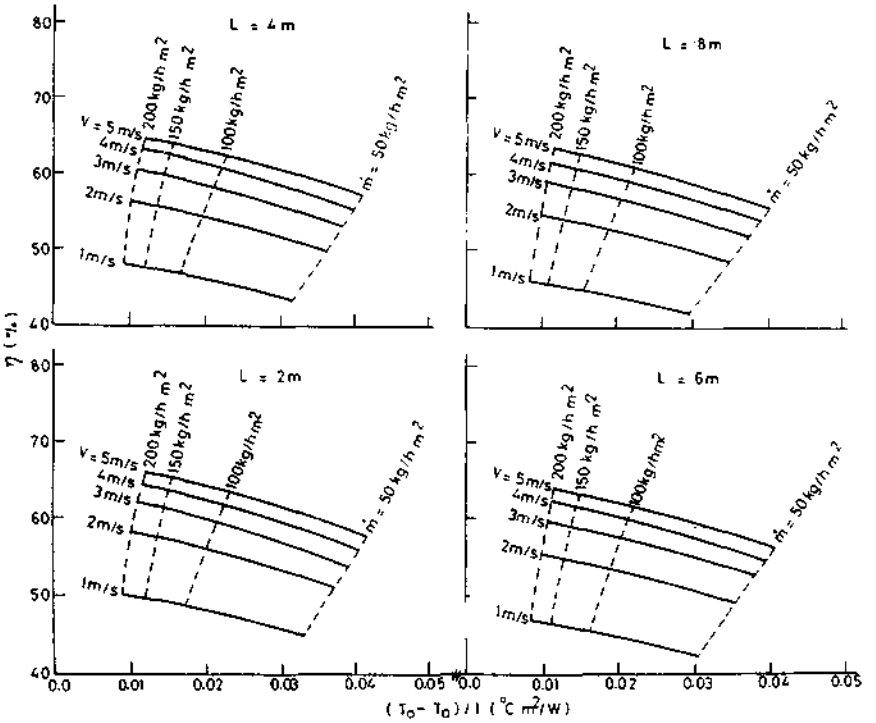

Fig. 8. Efficiency as a function of air temperature increment per unit incident flux for different air velocities in a Type V air heater.

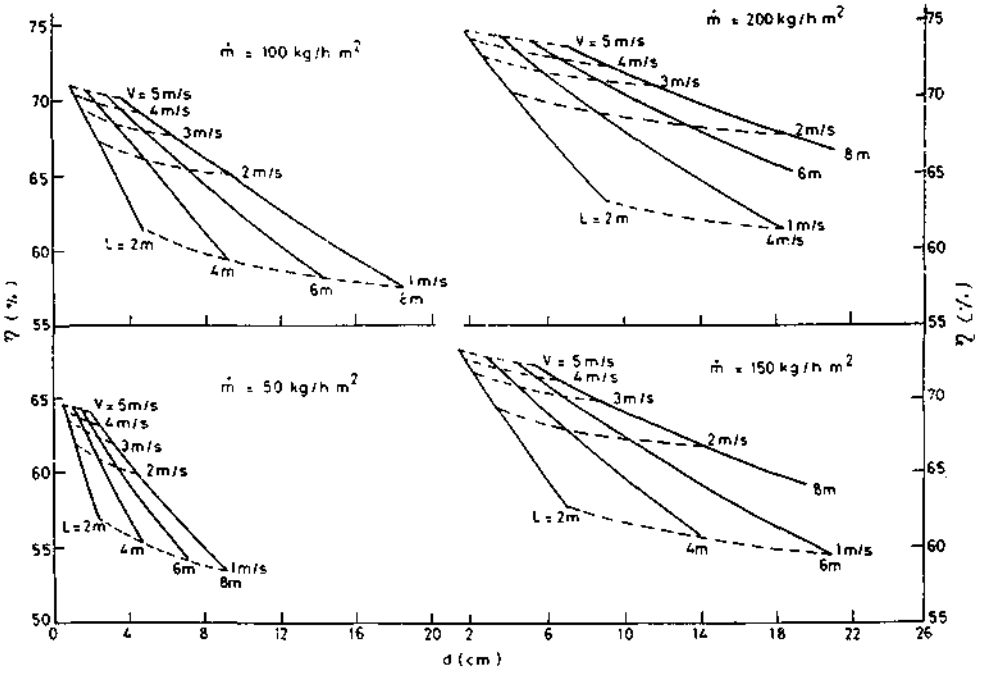

Fig. 9. Efficiency as a function of air channel depth for different air channel lengths of a Type I air heater.

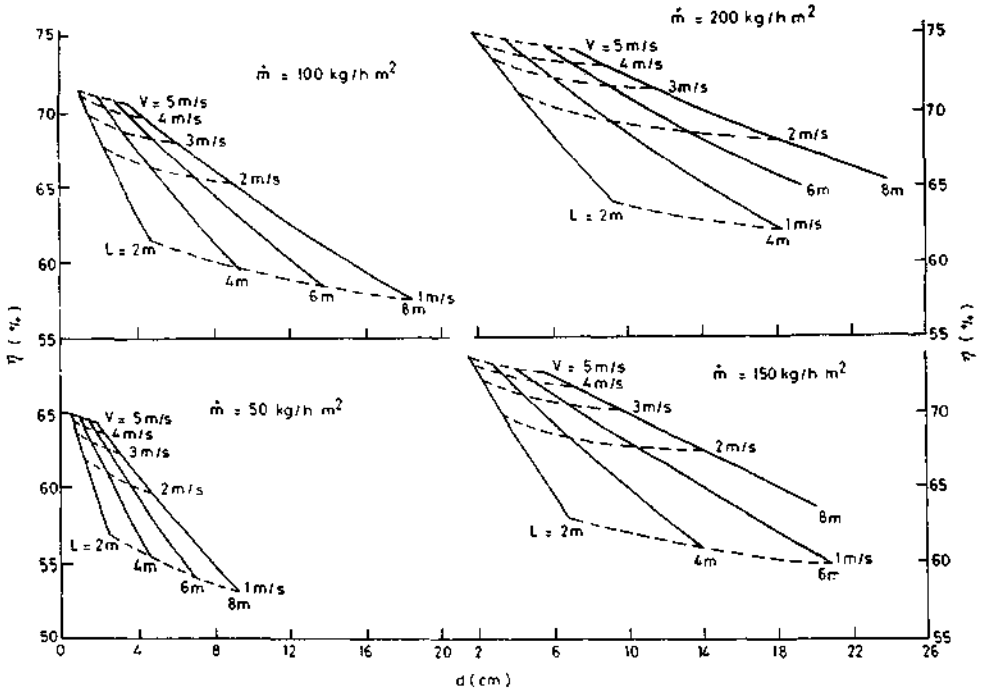

Fig. 10. Efficiency as a function of air channel depth for different air channel lengths of a Type II air heater.

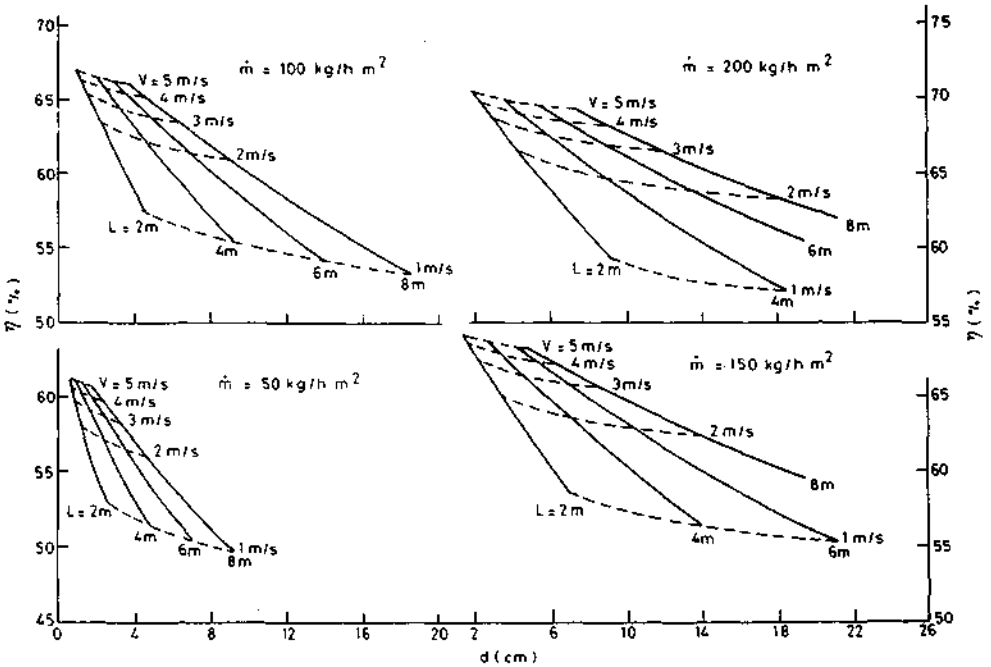

Fig. 11. Efficiency as a function of air channel depth for different air channel lengths of a Type III air heater.

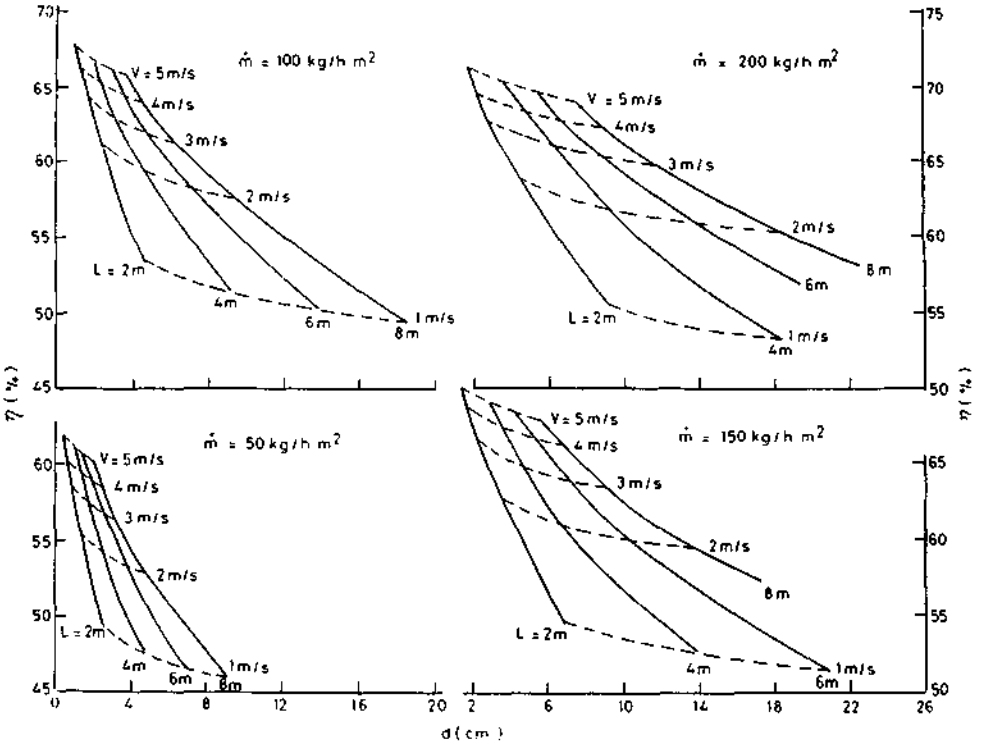

Fig. 12. Efficiency as a function of air channel depth for different air channel lengths of a Type IV air heater.

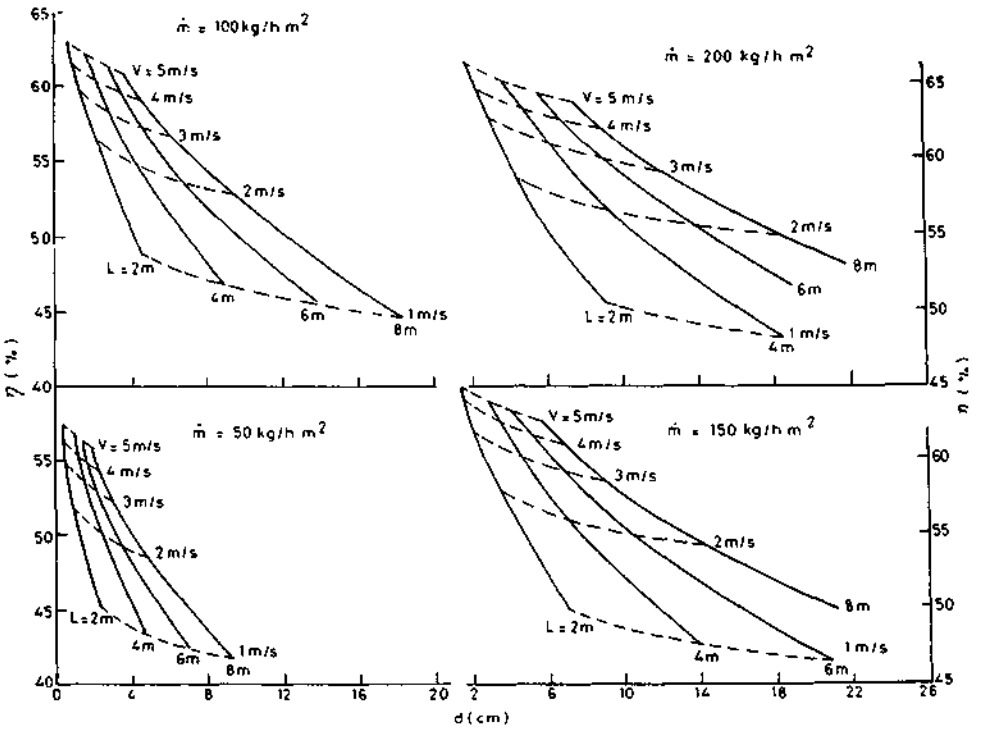

Fig. 13. Efficiency as a function of air channel depth for different air channel lengths of a Type V air heater.

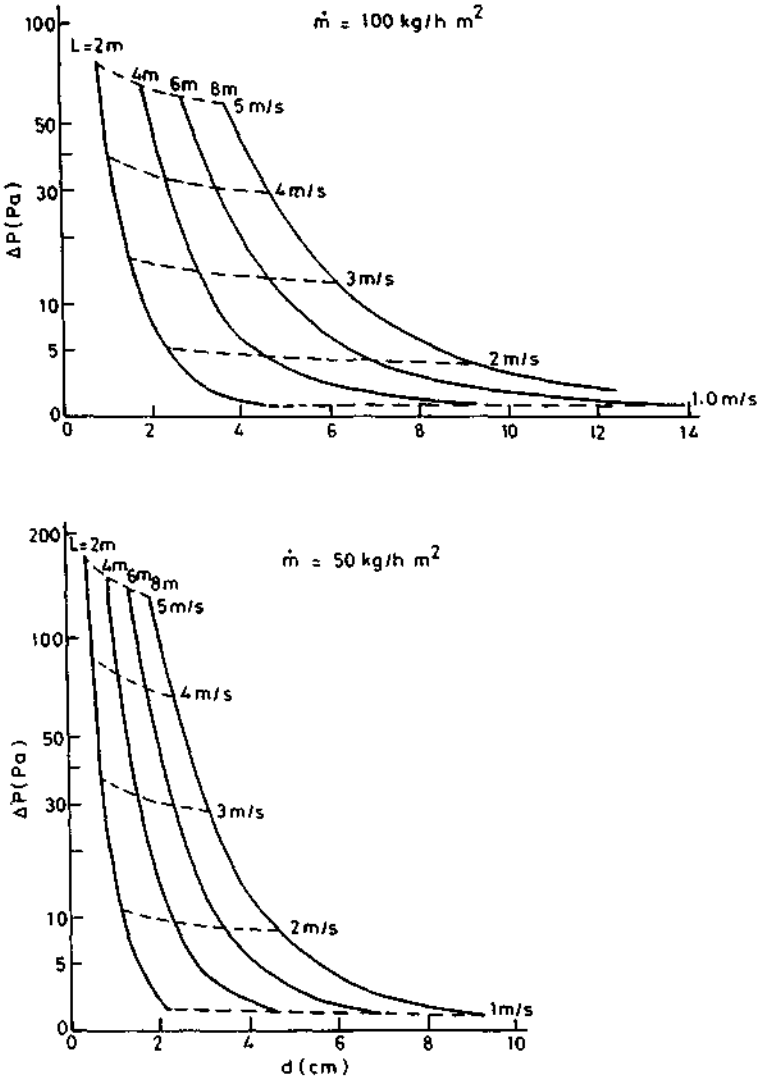

Fig. 14. Pressure drop as a function of air channel depth for different air channel lengths.

the width of the air heater should be fixed. Once the heater width is chosen, the air flow rate can be fixed by the requirement of the temperature increment level in the system. All other parameters being determined, the selection of the length and depth of the air channel can be made by the upper limit of the pressure drop experienced by the flowing air. For example, if the pressure drop is assumed fixed at a value of 30 Pa and the air flow rate at 200 kg/h m^2, then for flow channel lengths of 2, 4, 6 and 8 m, the channel depths should be chosen close to about 2, 3.6, 5.5 and 7.3 cm (Fig. 15), respectively. This would correspond to an efficiency of about 61% (Fig. 13) and an air temperature increment of about 0.013 K per unit incident intensity $(T_o - T_a)/I$ of solar radiation (Fig. 4). If the required air temperature increment level for a particular application is higher than this, for example, in the range of about 0.02–0.025 K m^2/W, which corresponds to a mass flow rate of 100 kg/h m^2 (Figs 4–8), for air channel lengths of 2, 4, 6 and 8 m, the air channel depths should be, respectively, (assuming a pressure drop of 30 Pa) 1.5, 2.5, 3.5 and 4.6 cm (Fig. 14) which would correspond to an efficiency of about 59–70% (Figs 9–13). In summary, by adopting a

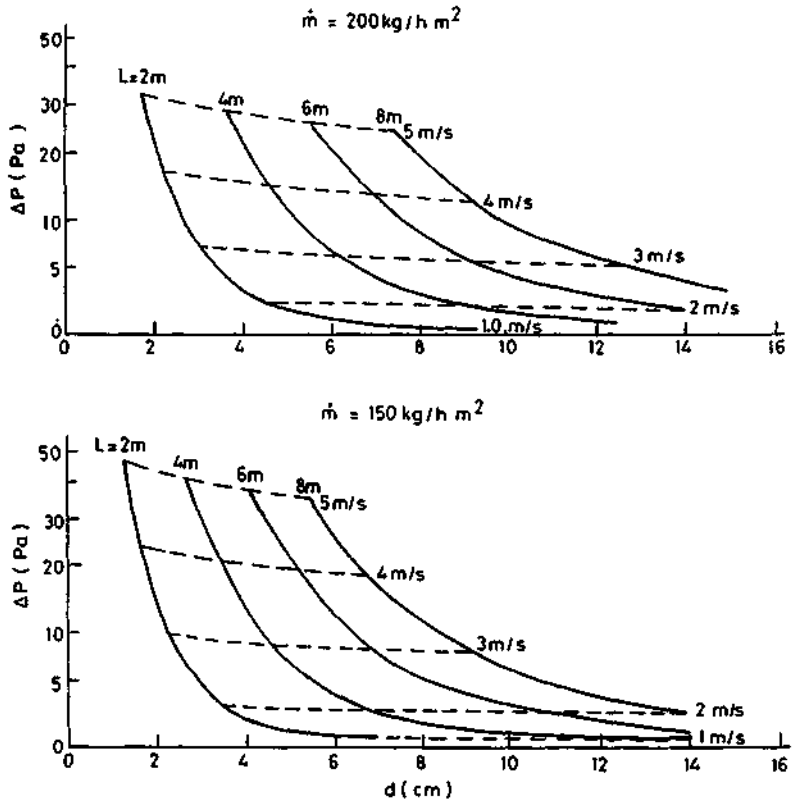

Fig. 15. Pressure drop as a function of air channel depth for different air channel lengths.

theoretical analysis and the curves discussed above, it would be possible to obtain economical and technically logical air heater designs.

4. CONCLUSIONS

Clearly, increasing the air velocity through the air heaters results in higher collection efficiency, but also in increased pressure drop. A reasonable compromising point can be determined by investigating the effects of various design and operational parameters on the efficiency, the air temperature increment and the pressure drop in the system and by adopting the method of design analysis discussed in the article. This process should be of interest to designers, engineers and consumers who like to compare the cost-effectiveness of commercial products.

NOMENCLATURE

- C specific heat capacity of air, Wh/kg °C
- d depth of air channel, m
- D equivalent diameter of air channel, m
- f friction factor
- h heat transfer coefficient, W/m² K
- I solar radiation incident on the collector, W/m²
- k thermal conductivity of air, W/m K
- L length of air heater, m
- $\dot{M}$ mass flow rate of air, kg/h
- $\dot{m}$ specific mass flow rate of air, kg/h m²
- M constant dependent of N
- N number of equivalent diameters
- Nu Nusselt number for any N
- Nu_∞ Nusselt number for fully developed thermal flow
- Pr Prandtl number
- Re Reynolds numbr
- V velocity of air flowing through the collector, m/s
- W width of absorber, m
- α solar absorptance of corrugated absorber
- β corrugation factor
- ΔP pressure drop experienced by the flowing air, Pa
- η efficiency of system
- μ dynamic viscosity of air, kg/m s
- ρ density of air, kg/m³

Suffix:

- a ambient
- f fluid

o outlet
1 upper plate
2 middle plate
3 bottom plate

REFERENCES

1. M. K. Seluck, *Solar Air Heaters and Their Applications in Solar Energy Engineering* (Edited by A. A. M. Sayigh). Academic Press, New York (1977).
2. G. O. G. Lof, *Solar Air Heating Systems in Solar Energy Conversion* (Edited by A. E. Dixon and J. D. Leslie). Pergamon Press, New York (1979).
3. J. A. Duffie and W. A. Beckman, *Solar Engineering Thermal Process*. John Wiley and Sons, New York (1980).
4. N. K. Bansal, R. Chandra and M. A. S. Malik, *Solar Air Heaters, Review of Renewable Energy Sources* (Edited by M. S. Sodha, S. S. Mathur and M. A. S. Malik). Wiley Eastern, India (1983).
5. W. W. S. Charters, Some aspects of flow duct design of solar air heating applications. *Solar Energy* **13**, 283 (1971).
6. K. G. T. Hollands and E. C. Schewen, Optimization of flow passage geometry for air heating plate-type solar collectors. *J. Solar Energy Engng, Trans. ASME* **103**, 323 (1981).
7. C. Choudhury, S. L. Andersen and J. Rekstad, A solar air heater for low temperature applications. *Solar Energy* **40**, 77 (1988).
8. H. M. Tan and W. W. S. Charters, Effect of thermal entrance region on turbulent forced convective heat transfer for an asymmetrically heated rectangular duct with uniform heat flux. *Solar Energy* **12**, 513 (1969).
9. H. Y. Wong, *Handbook of Essential Formula and Data on Heat Transfer for Engineers*. Longman, London (1977).

APPENDIX

$$P_1 = h_{1a}+h_{21}$$
$$P_2 = h_{21}+h_{23}+h_{2f}$$
$$P_3 = h_{21}^2/P_1$$
$$P_4 = P_3/h_{21}$$
$$P_5 = P_4 h_{1a}$$
$$P_6 = h_{23}+h_{3a}+h_{3f}$$
$$P_7 = h_{23}/(P_2-P_3)$$
$$P_8 = P_7 h_{23}$$
$$P_9 = P_7 h_{2f}$$
$$P_{10} = P_6-P_8$$
$$P_{11} = P_5 P_7+h_{3a}$$
$$P_{12} = P_9+h_{3f}$$
$$P_{13} = h_{2f}(S_2 I+S_1 I P_4+T_a P_5)/(P_2-P_3)$$
$$P_{14} = P_9+h_{3f}$$
$$P_{15} = h_{2f}^2/(P_2-P_3)-(h_{2f}+h_{3f})$$
$$P_{16} = P_{14}(S_3 I+S_2 I P_7+S_1 I P_4 P_7+T_a P_{11})$$
$$P_{17} = P_{12}P_{14}/P_{10}$$
$$P_{18} = P_{13}+P_{16}$$
$$P_{19} = P_{15}+P_{17}$$